Journal of the Korean Nuclear Society
Volume 27, Number 6, December 1995

A Generalized Model for the Prediction of Thermally-Induced CANDU Fuel Element Bowing

H.C. Suk, K-S. Sim, and J.H. Park
Korea Atomic Energy Research Institute
(Received March 27, 1995)

CANDU 핵연료봉의 열적 휨 모형 및 예측

석호천 · 심기섭 · 박주환
한국원자력연구소
(1995. 3. 27 접수)

Abstract

The CANDU element bowing is attributed to actions of both the thermally induced bending moments and the bending moments due to hydraulic drag and mechanical loads, where the bowing is defined as the lateral deflection of an element from the axial centerline. This paper considers only the thermally-induced bending moments which are generated both within the sheath and the fuel and sheath by an asymmetric temperature distribution with respect to the axis of an element. The generalized and explicit analytical formula for the thermally-induced bending is presented in consideration of 1) bending of an empty tube treated by neglecting the fuel/sheath mechanical interaction and 2) fuel/sheath interaction due to the pellet and sheath temperature variations, where in each case the temperature asymmetries in sheath are modelled to be caused by the combined effects of (i) non-uniform coolant temperature due to imperfect coolant mixing, (ii) variable sheath/coolant heat transfer coefficient, (iii) asymmetric heat generation due to neutron flux gradients across an element and so as to inclusively cover the uniform temperature distributions within the fuel and sheath with respect to the axial centerline. As the results of the sensitivity calculations of the element bowing with the variations of the parameters in the formula, it is found that the element bowing is greatly affected relatively with the variations or changes of element length, sheath inside diameter, average coolant temperature and its variation factor, pellet/sheath mechanical interaction factor, neutron flux depression factor, pellet thermal expansion coefficient, pellet/sheath heat transfer coefficient in comparison with those of other parameters such as sheath thickness, film heat transfer coefficient, sheath thermal expansion coefficient, and sheath and pellet thermal conductivities.

요 약

CANDU 핵연료봉의 휨은 열적 휨 모멘트와 수력학적 견인력 및 기계적 하중에 기인하는 휨 모멘트에

의하여 일어난다. 여기서, 연료봉 휨은 연료봉 축방향 중심선으로부터의 측면 처짐으로 정의한다. 본 논문에서는 연료봉 축방향 중심선에 대한 비대칭 온도분포에 의해 핵연료 피복관 자체와 피복관과 소결체의 상호작용 부위에서 발생하는 열적 휨만을 취급한다. 이를 위해 1) 소결체와 피복관 사이의 기계적 상호작용을 무시한 조건에서의 핵연료 피복관의 휨과 2) 소결체와 피복관의 온도 변화에 기인하여 발생하는 소결체와 피복관 사이의 기계적 상호작용을 고려한 조건에서의 연료봉 휨을 혼합 고려하고, 각각에서 피복관의 비대칭 온도분포가 (i) 냉각재의 불완전한 혼합에 따른 비균질 냉각재 온도, (ii) 핵연료 피복관과 냉각재 사이의 비균질한 열전달 계수, (iii) 핵연료내 반경 방향으로의 중성자속 감쇄에 의한 비대칭 열 발생 등의 복합적효과에 의해 발생되는 것으로 고려하여 피복관의 대칭온도 분포까지 포함할 수 있는 열적 휨의 일반적 해석 공식을 제시하였다. 본 휨 공식에 사용되는 모든 변수에 대한 민감도 분석을 통해, 핵연료봉 길이, 피복관 내경, 냉각재 평균 온도 및 변화 인자, 소결체－피복관 기계적 상호 작용 인자, 중성자속 감쇄 인자, 핵연료 열팽창 계수, 피복관-냉각재 열전도 계수 등의 변화가 피복관 두께, 피복관－냉각재 열전달 계수, 피복관 열팽창 계수, 핵연료-피복관 열전달 계수 등의 변화보다 핵연료봉의 열적 휨에 상대적으로 더욱 영향을 미치는 것으로 밝혀졌다.

1. Introduction

The element bowing of CANDU (Canada deuterium uranium) bundle as typically shown in Fig. 1 is defined as the lateral deflection of an element from the axial centerline.

Assessments of bowing of nuclear fuel elements can help demonstrate the integrity of fuel and of surrounding components, as a function of operating conditions such as channel power. Bowed fuel elements could reduce subchannel flow area resulting in poor heat transfer due to local coolant starvation and these elements may consequently defect as a result of local overheating. Another phenomenon which is attributed partially to bowing and partially. to irradiation induced swelling is the "sticking" of bundles in a fuel channel. If "sticking" occurs, more force is required during bundle shifting and removal during the refuelling process.

The element bowing is attributed to actions of both the thermally induced bending moments and the bending moments due to hydraulic drag and mechanical loads during the refuelling process, and is restrained by the appendages, end plates and neighboring elements of the bundle. Based on these phenomena, Veeder and Schankula[1] developed analytically a time-independent model of the thermally-induced bowing theory of CANDU type fuel elements. Their analysis was basically hypothesized that bowing of pelletized fuel elements of the type under consideration is primarily a thermally induced phenomenon. In further, based on this Veeder and Schankula model, Tayal[2] developed the BOW code to calculate the bowing of CANDU fuel elements due to gradients of temperature and due to hydraulic forces. It is noted that the variations of the coolant temperature and film heat transfer coefficient are neglected in their final formula for the element bowing, and that their formulas of the sheath temperature variations and so deflections are not adequately derived. To cope with these neglects and improper derivation of the bowing formula, an improvement of the bowing analysis model has been done through re-assessment of Veeder and Schankula model and so resulted in a generalized formula for the thermally-induced bowing calculation [3].

This paper describes the thermally-induced bending moments which are generated both within the sheath and the fuel and sheath by an asymmetric temperature distribution with respect to the axis of an element. One side of the element becomes hotter than the other and the element bows in the direction of the hotter side to accommodate the differential axial strain. As a time-independent model of the thermally-induced bowing theory, this paper presents the generalized and explicit analytical formulas in con-

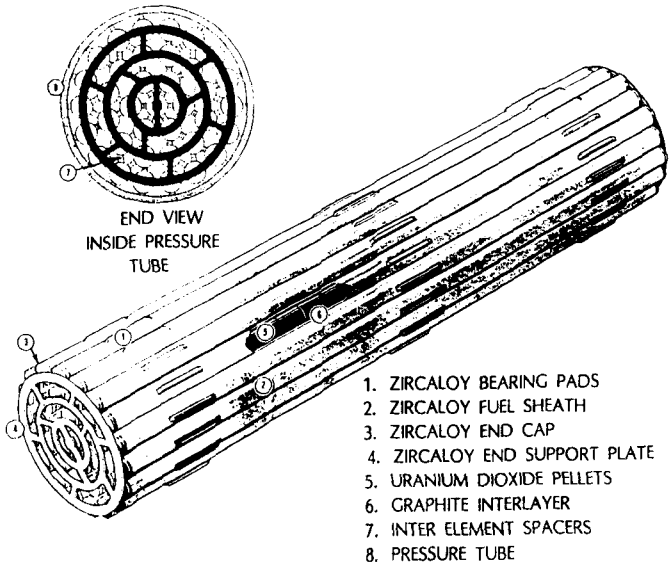

Fig. 1. 37-Element CANDU Fuel Bundle

sideration of 1) bending of an empty tube treated by neglecting the fuel/sheath mechanical interaction and 2) fuel/sheath interaction due to the pellet and sheath temperature variations. In each considerations, the temperature asymmetries in sheath are modelled to be caused by the combined effects of (i) non-uniform coolant temperature due to imperfect coolant mixing, (ii) variable sheath/coolant heat transfer coefficient, (iii) asymmetric heat generation due to neutron flux gradients across an element and so as to inclusively cover the uniform temperature distributions within the fuel and sheath with respect to the axial centerline. The thermally-induced bowing model is approached to calculate the temperature variations and hence the bending moments by considering the peripheral temperature gradients caused by them, since the temperature variations around the fuel and sheath set up the bend moments.

With the generalized model for the element bowing, a parametric study is carried out to investigate the influence of the variation or change of an element geometric, material or operation parameters such as one of element length, sheath inside diameter, coolant temperature variation factor, a factor of mechanical interaction between fuel pellet and sheath, neutron flux depression factor, pellet thermal expansion coefficient, pellet/sheath heat transfer coefficient, sheath thickness, film heat transfer coefficient, sheath thermal expansion coefficient, and sheath and pellet thermal conductivities on the element bowing.

Notation used in this paper are listed at the last page of this paper.

2. Analytical Modelling and Formulating of Bowing

2.1. Basic Hypotheses and General Solutions of Heat Conduction Equations

The model for the thermally-induced bowing of CANDU fuel elements presented in this paper is based on the three basic hypotheses from which the in-reactor bowing of pelletized fuel elements is considered to cause bending moments in the sheath due

to the sheath peripheral temperature gradients by:

(1) non-uniform coolant temperature due to imperfect coolant mixing,
(2) variable heat transfer coefficient between fuel and coolant, and
(3) asymmetric heat generation due to neutron flux gradients across an element.

The generalized and explicit analytical formula for the thermally-induced bending can be derived with consideration of 1) bending of an empty tube treated by neglecting the fuel/sheath mechanical interaction and 2) interaction between fuel pellet and sheath due to the pellet and sheath temperature variations.

The coordinate system used in the present model is shown in Fig. 2. The angle θ is measured in the clockwise direction from the vector CO. From the geometry of the bundle we make the plausible assumption that the temperature distributions within the fuel and sheath are symmetrical about the vector CO. It is also assumed that the neutron flux distribution through the bundle can approximately described by a modified Bessel function Io(κR), where κ is the inverse diffusion length for thermal neutrons in the homogenized fuel channel (fuel, coolant and sheath) and R is the displacement between the center of bundle and center of element under consideration. Using the Gegenbauer's addition theorem of Bessel functions [4], the modified Bessel function, Io(κR) permits solutions of the problem in the cylindrical coordinate system by analytical rather than numerical methods, i.e.,

$$I_0(xR) = I_0(xR_i)\, I_0(xr) + 2\sum_{m=1}^{\infty}(-1)^m I_m(xR_i)\, I_m(xr)\cos m\theta \quad (2.1-1)$$

If the fuel thermal conductivity, λ, is a constant value, the heat conduction equation in the fuel with asymmetric heat generation in the cylindrical coordinates becomes

$$\frac{1}{r}\frac{\partial}{\partial r}\left(r\frac{\partial T}{\partial r}\right)+\frac{1}{r^2}\frac{\partial^2 T}{\partial \theta^2}=-\frac{q_0}{\lambda}I_0(xR) \quad (2.1-2)$$

where q_0''' (r, R=0) is the power per unit volume at the centre of flux symmetry.

The heat conduction equation for the region of the sheath in which the heat generation is negligible is given by

$$\frac{1}{r}\frac{\partial}{\partial r}\left(r\frac{\partial T}{\partial r}\right)+\frac{1}{r^2}\frac{\partial^2 T}{\partial \theta^2}=0 \quad (2.1-3)$$

Since Eq.(2.1−2) can be rearranged to a Cauchy or Euler differential equation, a general solution to the heat conduction equation of Eq.(2.1−2) can be expressed as

$$T(r,\theta) = A_0 + A\, I_0(xR) + \sum_{m=1}^{\infty} A_m\, r^m \cos m\theta \quad (2.1-4)$$

where A_0 represents the centerline temperature, and A is given by

$$A=\frac{-q}{2\,\pi\,\lambda\,x\,a\,I_0(xR_i)\,I_1(xa)} \quad (2.1-5)$$

The general solution[5] of Eq.(2.1−3) as a form of Laplace equation for a plate which is bounded by two concentric circles of radius a and b can be obtain ed for the region of the sheath :

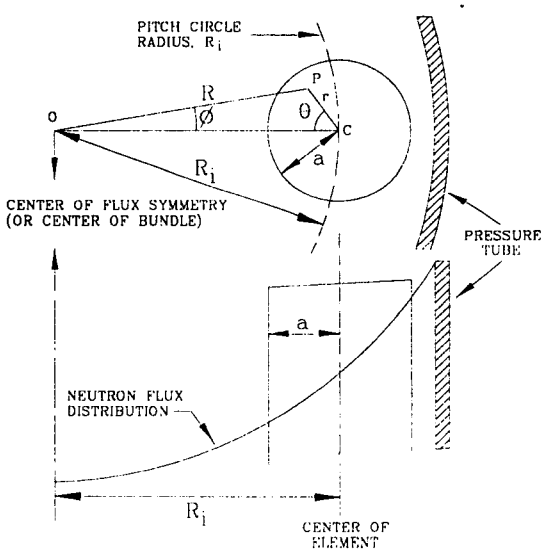

Fig. 2. Coordinate System Used in The Analysis

$$T_s(r,\theta) = B_0 + B \ln r + \sum_{m=1}^{\infty}\left(B_m r^m + \frac{C_m}{r^m}\right)\cos m\theta \quad (2.1-6)$$

2.2. Boundary Conditions of the Heat Conduction Equations

The coefficients in Eqs. (2. 1-4) and (2. 1-6) can be found by equating terms in cos mθ in the following boundary conditions for the asymmetric heat generating element in the non-uniform coolant temperatures due to imperfect mixing and non-uniform heat transfer between sheath and coolant :

(a) Coolant temperature variation at r=b:

$$T_c = \overline{T_c}(1 + \beta\cos\theta) \quad (2.2-1)$$

$$\text{where } \beta = \frac{T_c(\max) - T_c(\min)}{T_c(\max) + T_c(\min)} \quad (2.2-2)$$

(b) Continuity of heat flux at r=a :

$$\lambda \frac{\partial T}{\partial r}\Big|_{r=a} = \lambda_s \frac{\partial T_s}{\partial r}\Big|_{r=a} \quad (2.2-3)$$

$$-\lambda \frac{\partial T}{\partial r}\Big|_{r=a} = h_{fs}(T - T_s)\Big|_{r=a} \quad (2.2-4)$$

(c) Continuity of heat flux at r=b :

$$-\lambda \frac{\partial T_s}{\partial r}\Big|_{r=b} = h_{sc}(T_s - T_c)\Big|_{r=b} \quad (2.2-5)$$

where

$$h_{sc} = \overline{h_{sc}}(1 + \gamma\cos\theta) \quad (2.2-6)$$

$$\gamma = \frac{h_{sc}(\max) - h_{sc}(\min)}{h_{sc}(\max) + h_{sc}(\min)} \quad (2.2-7)$$

2.3. Formulation of Bowing

2.3.1. Bending of a Pellet/sheath Non-Mechanical Interacted Empty Tube

The fuel sheath can be treated as an empty tube, if the mechanical interaction between the sheath and fuel pellets is neglected. The empty tube bending moment due to temperature variation within the sheath can be found by using the following formula [6]

$$M_s = \alpha_s E_s \int_a^b \int_0^{2\pi} T_s \cos\theta\, r^2\, dr\, d\theta \quad (2.3-1)$$

which becomes

$$M_s \approx \frac{\pi \alpha_s E_s}{4}\left[B_1(b^4 - a^4) + 2C_1(b^2 - a^2)\right] \quad (2.3-2)$$

by substituting Eq.(2.1−6) with m=1 into Eq.(2. 3−1).

In a CANDU bundle, the end caps are welded to the ends of the sheaths to seal the elements. End plates are also welded to the end caps to hold the elements in the bundle assembly. So the sheaths can be assumed in hinged end conditions. Therefore, the deflection δ of the sheath at the mid-span due to the bending moment is given by

$$\delta \approx \frac{M_s l^2}{8 E_s I_s} = \frac{l^2 \alpha_s}{8 b}\left[B_1 b + \frac{C_1}{b}\right] \quad (2.3-3)$$

in which $I_s = \pi(b^4 - a^4)/4$ is used for the moment of inertia, I_s, of a hollow tube of thickness t=b−a and then t/b≈0 is counted for the thinned walled tube. Veeder and Schankula[1] noted that the hinged end condition has been found experimentally to be a good approximation for elements in the type of fuel bundles under investigation at AECL.

Since the maximum surface temperature of sheath is given by setting m=1 and θ=0 or 2π in Eq.(2. 1−6), and the minimum surface temperature of sheath is given by setting m=1 and θ=π in Eq.(2. 1−6), the bracketed term in Eq.(2.3−3) is reduced to be approximately equal to half of the difference between the maximum ($T_{s,max}$) and minimum ($T_{s,min}$) surface temperatures of sheath :

$$B_1 b + \frac{C_1}{b} \approx \frac{T_{s,max} - T_{s,min}}{2} \equiv \frac{\Delta T_s}{2} \quad (2.3-4)$$

where B_1 and B_2 are determined by applying the boundary conditions in Section 2.2.

Cooperating Eqs.(2.1−4) and (2.1−6) with the boundary conditions in Session 2.2 where m = 1 shall be provided, as detailed in the reference 3, the half of the difference between the maximum and minimum surface sheath temperatures is obtained as

$$\left(B_1 b + \frac{C_1}{b}\right) = \{a K_1 [\ \overline{h_{sc}}(1 - \gamma^2) \beta \overline{T_c} - \gamma \overline{w}\ ] - 2 b \overline{w} D\}/K_2 \quad (2.3-5)$$

This equation gives the difference ΔT_{SE} between the maximum and minimum surface temperatures of sheath according to Eq. Eq.(2.3−4), and the deflection δ_{SE} of the empty tube according to Eq.(2.3−3):

$$\Delta T_{SE} \approx 2\{a K_1 (\overline{h_{sc}}(1 - \gamma^2) \beta \overline{T_c} - \gamma \overline{w}) - 2 b \overline{w} D\}/K_2 \quad (2.3-6)$$

$$\delta_{SE} \approx \frac{l^2 \alpha_s}{8 b K_2} \{a K_1 (\overline{h_{sc}}(1 - \gamma^2) \beta \overline{T_c} - \gamma \overline{w}) - 2 b \overline{w} D\} \quad (2.3-7)$$

where

$$K_1 = 1 + \frac{\lambda}{a h_{fs}} + \frac{\lambda t}{a \lambda_s} \quad (2.3-8)$$

$$K_2 = \lambda + a \overline{h_{sc}}(1 - \gamma^2)\left(1 + \frac{\lambda}{a h_{fs}} + \frac{\lambda t}{a \lambda_s}\right) \quad (2.3-9)$$

$$\overline{w} = \frac{q}{2 \pi b} \quad (2.3-10)$$

$$D = \frac{I_1(x R_i)\, I_2(x a)}{I_0(x R_i)\, I_1(x a)} \quad (2.3-11)$$

in which $\overline{w}$ is the average heat flux of the element and D is a factor determined by the flux depression through the fuel bundle.

2.3.2. Bending Due to Interaction Between Pellet Stack and Sheath

The fuel pellet stack is a column of ceramic fuel pellets within the sheath. Each of the pellets cracks into many smaller pieces during irradiation. The fuel stack is therefore incapable of sustaining an applied bending moment. If, however, the sheath is collapsed into the pellets or the fuel grips the sheath, it can induce a bending moment in the sheath, because the thermal expansion of the sheath at the interface is smaller than that of the pellet. Assuming that the strength of the sheath is insufficient to resist the thermal expansion of the fuel, the component of strain due to the elastic stress in the sheath can be ignored. Based on this assumption, at the point (a, θ), the difference in longitudinal thermal strain between the fuel and sheath is given by

$$\Delta S(a, \theta) = \alpha T(a, \theta) - \alpha_s T_s(a, \theta) \quad (2.3-12)$$

and

$$T(a, \theta) - T_s(a, \theta) = -\frac{\lambda}{h_{fs}} \frac{\partial T}{\partial r} \Big|_{r=a} \quad (2.3-13)$$

which is provided by Eq.(2.2−4). If there is no slip between fuel stack and sheath, the sheath will be strained in the axial direction by an amount equal to the differential thermal strain, and if there is some slip between them, the mechanical strain will be less than the differential thermal strain. Therefore, a relationship between the differential thermal strain and the induced mechanical strain can be expressed by

$$\Delta\varepsilon(a, \theta) = G \Delta S(a, \theta) \quad (2.3-14)$$

where G is a factor between 0 and 1. Substituting Eqs. (2.3−12) and (2.3−13) into Eq.(2.3−14) gives

$$\Delta\varepsilon(a, \theta) = G\left\{[\ (\alpha - \alpha_s)\ T(a, \theta)] - \frac{\lambda \alpha_s}{h_{fs}} \frac{\partial T}{\partial r} \Big|_{r=a}\right\} \quad (2.3-15)$$

Predictions with the CANDU fuel modelling code ELESTRES[10] indicate that, for a free standing sheath having a diametral clearance of 0.08mm, G is about 0.5. Clearly, the collapsibility of the sheath implies a value of G greater than 0.5.

Also, cooperating Eqs.(2.1−4) and (2.1−6) with the boundary conditions at r = a and m = 1, the strain relationship of Eq.(2.3−15) is given by

$$\Delta\varepsilon(a,\theta) \approx G\left\{K_3\,\overline{T_c}\,(1+\beta\cos\theta) - Z + K_4\left[\left(\frac{\lambda\gamma\,\overline{w}-2\,\overline{h_{sc}}\,(1-\gamma^2)\,b\,\overline{w}\,D}{K_2}\right) - \beta\,\overline{T_c}\left(\frac{\lambda\,\overline{h_{sc}}\,(1-\gamma^2)}{K_2}\right)\right]\cos\theta\right\} \quad (2.3-16)$$

where

$$K_3 = \alpha - \alpha_s \quad (2.3-17)$$

$$K_4 = (\alpha - \alpha_s)\left(\frac{1}{h_{fs}} + \frac{t}{\lambda_s} + \frac{1}{h_{fs}}\right) + \frac{\alpha_s}{h_{fs}} \quad (2.3-18)$$

$$Z = A\,\lambda\,K_4\,x\,I_0(x R_i)\,I_1(x a)$$

Cooperating Eq.(2.3−16) with Eq.(2.3−1), the induced bending moment in the sheath is given by

$$M_s = E_s\,a^2\,t\int_0^{2\pi}\Delta\varepsilon(a,\theta)\,\cos\theta\,d\theta \quad (2.3-19)$$

It is noted that terms in the integrand of Eq.(2.3−19) which are independent of θ vanish when integrated between the limits, as do all terms in cos θ. Also assuming the hinged end conditions, δ_{SI} the deflection dSI due to the induced bending moment at the mid-span is given by

$$\delta_{SI} \approx \frac{M_s l^2}{8E_s I_s} \approx \frac{Gl^2}{8a}\left\{\beta\overline{T_c}\left(K_3 - \frac{K_4\,\lambda\,\overline{h_{sc}}\,(1-\gamma^2)}{K_2}\right) + \frac{K_4\overline{w}\,(\lambda\gamma-2\overline{h_{sc}}\,(1-\gamma^2)bD)}{K_2}\right\} \quad (2.3-20)$$

$$= \frac{l^2 a_s}{16b}\left\{\frac{2Gb}{a a_s}\left(\beta\overline{T_c}\left(K_3 - \frac{K_4\,\lambda\overline{h_{sc}}\,(1-\gamma^2)}{K_2}\right)\right) + \frac{K_4\overline{w}\,(\lambda\gamma-2\overline{h_{sc}}\,(1-\gamma^2)bD)}{K_2}\right\} \quad (2.3-21)$$

in which the moment of inertia, $I_S = \pi\,a^3\,t$ has been used for thin walled tubing.

Noting Eqs.(2.3−6) and (2.3−7), the term in the brackets of the Eq.(2.3−21) may arbitrarily be regarded as being equivalent to a temperature difference, ΔT_{SI}, across the sheath which would produce a deflection equal to that caused by interaction between fuel pellet and sheath. Thus,

$$\Delta T_{SI} \approx \frac{2Gb}{a a_s}\left\{\beta\overline{T_c}\left(K_3 - \frac{K_4\lambda\overline{h_{sc}}\,(1-\gamma^2)}{K_2}\right) + \frac{K_4\,\overline{w}(\lambda\gamma-2\overline{h_{sc}}\,(1-\gamma^2)bD}{K_2}\right\} \quad (2.3-22)$$

2.3.3. Bending Due to the Combined Effects of the Pellet/Sheath Non-Mechanical and Mechanical Interactions

In Session 2.3.2, the element bowing at the point (a, θ) is due to the difference in longitudinal thermal strain between the fuel and sheath for the interaction between pellet stack and sheath. This element bowing does not include the effect of the bending moment due to temperature variation within the sheath as treated in Session. 2.3.1. So the element bowing due to the combined effects of the non-mechanical and mechanical interactions between the pellet and sheath shall be formulated by adding the results together from Sessions 2.3.1 and 2.3.2 :

$$\Delta T_{SC} \approx \frac{2\{aK_1(\overline{h_{sc}}\,(1-\gamma^2)\beta\overline{T_c}-\gamma\overline{w})-2b\overline{w}D\}}{K_2} + \frac{2Gb}{aa^2}\left\{\beta\overline{T_c}\left(K_3 - \frac{K_4\lambda\overline{h_{sc}}\,(1-\gamma^2)}{K_2}\right) + \frac{K_4\,\overline{w}\,(\lambda\gamma-2\,\overline{h_{sc}}\,(1-\gamma^2)bD)}{K_2}\right\} \quad (2.3-23)$$

which is given by adding Eq.(2.3−6) with Eq.(2.3−22), and

$$\delta_{sc} \approx \frac{l^2 a_s\{aK_1(\overline{h_{sc}}\,(1-\gamma^2)\beta\overline{T_c}-\gamma\overline{w})-2b\overline{w}D\}}{8bK_2} + \frac{Gl^2}{8a}\left\{\beta\overline{T_c}\left(K_3 - \frac{K_4\lambda\overline{h_{sc}}(1-\gamma^2)}{K_2}\right)\right.$$

$$+\frac{K_4\overline{w}\ (\lambda\gamma-2\overline{h_{sc}}\ (1-\gamma^2)bD)}{K_2}\Bigg\} \quad (2.3-24)$$

which is given by adding Eq.(2.3−7) with Eq.(2.3−20).

3. Discussion

During irradiation of fuel bundles in CANDU reactor, the radial distributions of neutron flux and subchannel coolant temperatures through a fuel bundle are considered to be symmetrical about the bundle axis centerline. So, the neutron flux distribution through the center element and subchannel coolant temperature distribution around the element periphery will be symmetrical about the element axis centerline. However, the neutron flux distribution through the other element such as any one of the elements located at outer, intermediate and inner rings of the bundle and subchannel coolant temperatures around the element periphery will be asymmetrical about the element axis centerline. Therefore, a generalized model for predicting element bowing is required for the application of a fuel element subjected to all the symmetric and/or asymmetric thermal boundary conditions. Eqs.(2.3−23) and (2.3−24) represent the generalized and explicit analytical formulas for the time-independent predictions of the thermally-induced bowing of CANDU fuel elements. These formulas take into account the influences of the temperature asymmetries which are caused by (i) non-uniform coolant temperature due to imperfect coolant mixing, (ii) variable sheath/coolant heat transfer coefficient, (iii) asymmetric heat generation due to neutron flux gradients across an element. It is noted that Eqs.(2.3−6), (2.3−16) and (2. 3. -22) are comparable with Veeder and Schankula's equations (11), (16) and (20) in Reference 1, respectively, where Veeder and Schankula's equations (11) and (20) do not take into account the effects of the coolant temperature and film heat transfer coefficient variations, and Veeder and Schankula's equations (11) and (16) can not be obtained even if using their assumptions.

To illustrate the relative importance of the various parameters affecting fuel element bowing, the quantities of the sheath temperature difference, ΔT_{sc} of Eq. (2.3−23), and the element deflection, δ_{sc} of Eq.(2.3−24), are calculated for the fuels in three kinds of heavy water moderated reactors. The first is the natural UO_2 fuel sheathed in Zircaloy for CANDU-6 reactor[7]. The second[1] is the natural UO_2 fuel sheathed in Zircaloy for the Douglas Point 200 MW(e) power reactor which was cooled by pressurized heavy water, and the third[1] is the driver fuel of enriched UO_2 fuel sheathed in Zr-2.5wt% Nb for the AECL WR-1, an organic-cooled research reactor. In all the reactors, the moderator is kept cool and all the fuel bundles are contained in zirconium alloy pressure tubes. In each case, the calculations refer to an element in the outer ring of a bundle. The numerical values of the pertinent parameters are given in Table 1. The parameter values are taken to explain bowing in CANDU type fuel elements without having to invoke other mechanisms such as compressive axial loads. For the CANDU-6 fuel parameters valued in Table 1, the average coolant temperature, $\overline{T_c}$ and the fractions, β and γ are estimated for the N-6 highest power channel of Wolsong-1 reactor, using the thermal-hydraulic code, COBRA[8], where β and γ parameters are dependent on the coolant temperatures in the coolant subchannels of the bundle. The element linear power q′ and the neutron flux depression factor D are evaluated with the physics code of WIMS-AECL [9], where q′ and D parameters are mainly dependent on the fuel enrichment and burnup for a given reactor operational conditions and are taken in consideration of the reference high power envelope [7]. The sheath and fuel thermal expansion coefficients α_s and α, the sheath and fuel thermal conductivities λ_s and λ, and the heat transfer coefficient, h_{fs}, between fuel and sheath are evaluated with the CAN D are evaluated with the physics code of WIM-AECL [9], where q′ and D parameters are mainly materials chosen in the element design and are

Table 1. Numerical Values* of Fuel Element Parameters used for Calculations in Chapter 3

Parameter	Douglas Point [1]	WR-1 [1]	CANDU-6 Fuel Element
a(mm)	7.2	7.2	6.12
t(mm)	0.4	0.68	0.42
l(mm)	500	500	500
D(fraction)	0.032	0.07	0.030
q′ (kW/m)	50.0	46.5	51.6
α_s (μm/m K)	6.5	6.4	4.4
α(μm/m K)	11.0	11.0	11.0
λ_s(kW/mK)	0.013	0.013	0.016
λ(kW/mK)	0.003	0.003	0.003
	50.0	13.0	50.0
γ(fraction)	0.0	0.0	0.026
h_{fs}(kW/m^{2}K)	10.0	10.0	9.86
	280	350	300
β(fraction)	0.0	0.0	0.0048
G(fraction)	1.0	1.0	1.0

* The values are assumed for the present calculations to explain bowing in CANDU type fuel elements without having to invoke other mechanisms such as compressive axial loads.

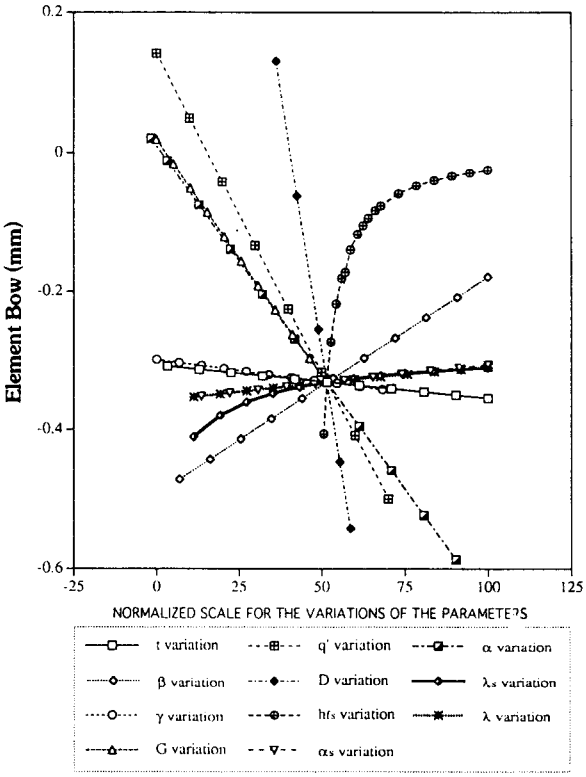

Fig. 3. The Bow Sensitivity of the Asymmetric Heat Generated Element With the Variations of the Parameters (37-Element Bundle in Table 1)

usually given as a function of the material temperature.

The sensitivities of the parameters employed in (2.3−24) are shown in Figs. 3 and 4 respectively for the asymmetric and symmetric heat generating fuel elements, where the variation or change was made for each one of β, λ, G, q′, h_{fs}, α_s, α, λ_s and λ and t in the equation for all the other fixed parameters of CANDU-6 fuel element in Table 1. In Figs. 3 and 4, the vertical axis represents the deflections of the elements at the mid-span and the negative or positive value of the deflections refers to the element deflection in direction of the pressure tube wall side or the bundle center side. The horizontal axis represents a normalized scale, N, for the variation or change of each one of the parameters where N=51.6 corresponds to each the values of the CANDU-6 fuel parameters in Table 1.

3.1. Influence of the Pellet/Sheath Interaction Term and G Change on the Bowing

For the instance of CANDU-6 fuel element characterized in Table 1, the bending due to the empty tube term as the first term in the right hand side of Eq.(2.3−24) resulted in 0.02mm towards the bundle center since the sheath outer surface temperature in fuel bundle center side is more hotter than that in the pressure tube wall side because of the hotter coolant temperature in the bundle center side, while the bending due to the pellet/sheath interaction term as the second term of the right hand side resulted in 0.35mm towards the pressure tube wall since the sheath inner surface temperature in the pressure

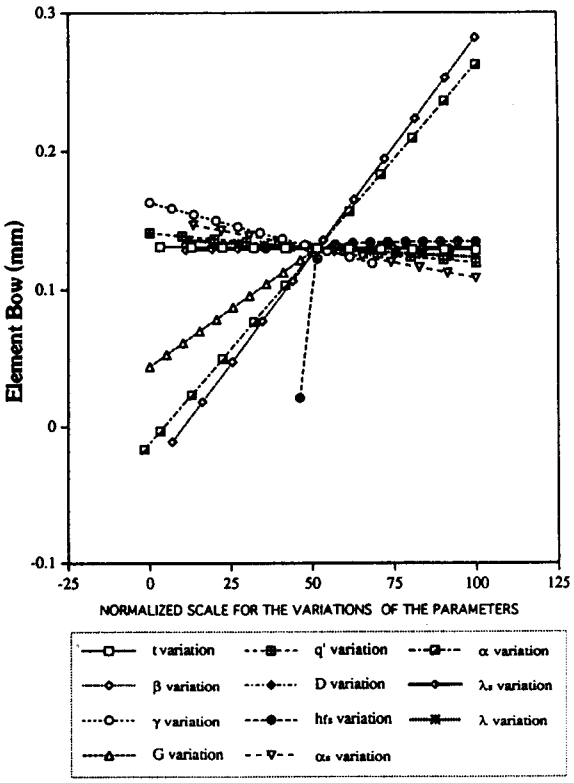

Fig. 4. The Bow Sensitivity of the Symmetric Heat Generated Element With the Variations of the Parameters (37-Element Bundle in Table 1)

tube wall side is more hotter than that in the fuel bundle center side because of the small neutron flux gradients in the pressure tube wall side, and, therefore, the net bending resulted in 0.33mm towards the pressure tube wall. The mechanical interaction between the pellet stack and the sheath has, in this instance, about 18 times greater effect on the element bowing than the empty tube as in the non-interaction between the pellet and the sheath. Since the pellet/sheath interaction predominates, there will be a tendency for the element in the bundle to bow out towards the wall of the pressure tube. Also, it can be realized that the bending will be increased almost directly in proportion to the square of the element length l, and almost in inverse proportion to the inner radius a of sheath as can be realized from the above comparison between the pellet/sheath interaction and non-interaction terms. Changing with G= 0.0 to+1.0 only in Eq.(8.1−24), the deflection of CANDU-6 asymmetric or symmetric heat generated element was significantly increased as expected as a linear function with the increase of G=0.0 to+1.0 as shown in Figs. 3 and 4, where their deflections were in the opposite directions between each other. So, if the element has a mechanical interaction between the pellet stack and sheath, the bending will be increased almost in proportion to the mechanical interaction factor G.

3.2. Influence of the Asymmetric or Symmetric Heat Generation in the Elements

Figs. 3 illustrates that a CANDU-6 fuel element generated asymmetric heat with respect to the central axis ($D \neq 0$) will bow out towards the wall of the pressure tube since the neutron flux gradient across the element is more affected in the bowing. However, if the element generated symmetric heat with respect to the central axis ($D=0$), the elements will bow out towards the center of bundle as shown in Fig. 4 because of the hotter coolant temperature in the bundle center side.

3.3. Sensitivities of the β and γ Variations on the Bowing

According to the COBRA[8] predictions for the CANDU-6 37-element bundle in the single phase flow region of the coolant, the β value for the outer elements as shown in Table 1 is almost monotonously increased from almost zero of the first bundles located at the upstream in the fuel channel to 0.0048 of the ninth bundle from the upstream, and the γ value is resulted in −0.014 for the first bundles located at the upstream and varied in the range of 0.014 to 0. 026 in the region of the second through ninth bundles.

For the outer element of the first CANDU-6 bun-

dle with $\beta=0.0001$ and $\gamma=-0.014$, Eq.(2.3−24) estimated the thermally-induced element bowing of $\delta_{SC}\approx 0.45$mm towards the pressure tube wall, provided with $\Delta T_{SC}\approx 43.0$K estimated by Eq.(2.3−23). If no variations of coolant temperature and film heat transfer coefficient around the periphery of the element, $\beta=0.0$ and $\gamma=0.0$, are existed, the bowing of $\delta_{SC}\approx$ 0.46mm towards the pressure tube wall side will be induced thermally, provided with $\Delta T_{SC}\approx 43.9$K.

Also using the equations for the element of the ninth CANDU-6 bundle with $\beta=0.0048$ and $\gamma=0.026$, the thermally-induced element bowing was estimated as 0.33mm in the direction of the pressure tube wall side, provided with $\Delta T_{SC}\approx 31.5$K. This element bowing was reduced as much as about 40% in comparison with that with $\beta\approx 0$ and $\gamma\approx 0$. With the increase of β value only in Eq.(2.3−24), the bowing of CANDU-6 asymmetric ($D\neq 0$) or symmetric ($D=0$) heat generated elements was stiffly and linearly decreased as shown in Figs. 3 and 4. Therefore, there will be significantly different results of the element deflections due to the variation of β value. Changing with the average coolant temperature $\overline{T_c}$ only, Eq.(2.3−24) results that the deflections of the asymmetric and symmetric heat generating elements will behavior in the same for the β value only.

With the increase of γ value only in Eq.(2.3−24), the bowing of CANDU-6 asymmetric heat generated element was slowly and linearly increased as shown in Fig. 3, and the bowing of the symmetric heat generated elements, however, was slowly and linearly decreased as shown in Fig. 4. So it can be noted that the effect of the γ variation on the element bowing is not greater than that of β variation.

3.4. Influence of the q′ and D Changes on the Bowing

With the increase of q′ value only in Eq.(2.3−24), the bowing of CANDU-6 asymmetric heat generated element ($D\neq 0$) was significantly and linearly increased as shown in Fig, 3, and however, the bowing of the symmetric heat generated element ($D=0$) was slowly and linearly decreased as shown in Fig. 4.

With the increase of neutron flux depression factor D value only in Eq.(2.3−24), the bowing of CANDU-6 asymmetric heat generated element was stiffly and linearly increased as shown in Fig. 3. However, if the element has no neutron flux depression, $D=0.0$ such as in the fuel element with the symmetric heat generation, the element was in a constant deflection in the direction of the bundle center side as expected.

3.5. Influence of the h_{FS}, a_s, a, λ_s, λ and t Changes on the Bowing

With the increase of h_{fs} value only in Eq.(2.3−24), the bowing of CANDU-6 asymmetric heat generated element was exponentially decreased as shown in Fig. 3 in which the element bowing is decreased with a rather stiff slope for the range of $h_{fs}=0.001$ to about 30 kW/m^{2}K, while the element bowing is decreased with a rather flattened slope for the range of hfs = about 30 to 90kW/m^{2}K.

With the increase of α value only in Eq.(2.3−24), the bowing of CANDU-6 asymmetric or symmetric heat generated element was slowly and linearly reduced as shown in Figs. 3 and 4.

With the increase of λ_s value only in Eq.(2.3−24), the bowing of the asymmetric or symmetric heat generated elements was stiffly and linearly increased as shown in Figs. 3 and 4.

With the increase of l_s value only in Eq.(2.3−24), the bowing of CANDU-6 asymmetric heat generated element was stiffly and exponentially decreased as shown in Fig. 3, while the bowing of CANDU-6 symmetric heat generated element was slowly and exponentially decreased as shown in Fig. 4.

With the increase of l value only in Eq.(2.3−24), the bowing of CANDU-6 asymmetric or symmetric heat generated element was slowly and linearly decreased as shown in Figs. 3 and 4.

With the increase of sheath thickness t only in Eq. (2.3-24), the bowing of CANDU-6 asymmetric heat generated elements was slowly and linearly raised in the direction of the pressure tube wall as shown in Fig. 3 because of the hotter temperature of sheath inner surface in the pressure tube wall side, and the bowing of CANDU-6 symmetric heat generated elements, however, was slowly and linearly reduced in the direction of the bundle center as shown in Fig. 4 because of the hotter coolant temperature in the bundle center side.

3.6. Bowing Prediction of WR-1 and Douglas Point fuel Elements

As shown in Table 1 of the parameter characteristics for the Douglas Point and WR-1 asymmetric heat generated fuel elements with $\beta=0$ and $\gamma=0$, Eqs.(2.3-23) and (2.3-24) estimated that, for the Douglas Point fuel element, $\Delta T_{sc} \approx 31.4K$ and $\delta_{sc} \approx 0.42mm$ towards the pressure tube wall; for the WR-1 fuel element, $\Delta T_{sc} \approx 94.6K$ and so $\delta_{sc} \approx 1.22mm$ towards the pressure tube wall side. The bowing prediction for WR-1 fuel element is ordered within the experimental results of the fuel elements [1].

4. Conclusions

(1) The present formula of Eqs.(2.3-23) and (2.3-24) represent the generalized and explicit analytical equations for the predictions of the thermally induced element bowing. It is noted that Eqs.(2.3-6), (2.3-16) and (2.3.-22) are comparable with Veeder and Schankula's equations (11), (16) and (20) in Reference 1, respectively, where Veeder and Schankula's equations (11) and (20) do not take into account the effects of the coolant temperature and film heat transfer coefficient variations, and Veeder and Schankula's equations (11) and (16) can not be obtained even if using their assumptions.

(2) For the elements such as the outer elements of the first bundle at the upstream in the CANDU-6 fuel channel, the deflections of an asymmetric heat generating element may be conservatively estimated by $\beta \approx 0$ and $\gamma \approx 0$ in Eq.(2.3-24), according to the COBRA code prediction.

(3) A CANDU asymmetric heat generating fuel elements ($D \neq 0$) will bow out towards the wall of the pressure tube, while a CANDU symmetric heat generating fuel elements ($D=0$) will bow out towards the center of bundle in the non-uniform distribution(s) of the coolant temperatures and/or the film heat transfer coefficients at the periphery of the elements.

(4) In Eq.(2.3-24), the pellet/sheath mechanical interaction has very greater effect on the element bowing than the empty tube. Since the pellet/sheath interaction predominates, there will be a tendency for the element in the bundle to bow out towards the wall of the pressure tube. So, the bending will be increased almost in proportion to the pellet/sheath interaction factor G as well as to the square of the element length l, and almost in inverse proportion to the inner radius a of sheath. It is noted that G is an empirical factor and so it is required to find appropriate value by experiments or computer simulation with existing irradiation data in a long term.

(5) With the increase of the sheath thickness only, the bowing of CANDU asymmetric heat generating elements will be slowly and linearly raised, and, however, the bowing of the symmetric heat generated elements will be slowly and linearly reduced.

(6) The deflection of the asymmetric or symmetric heat generating elements will be stiffly and linearly reduced with the increase of β value only, and, however, will be slowly and linearly raised with the increase of γ value only. So, there will be significant difference in the element deflections with the variation of β value only and the effect of the γ variation on the element bowing is not greater than that of β variation.

(7) With the increase of q′ value only, the bowing of the asymmetric heat generating elements ($D \neq 0$) will be stiffly and linearly raised, and, however, the bowing of the symmetric heat generating element ($D = 0$) will be slowly and linearly decreased. With the increase of D value only, the bowing of the asymmetric heat generating element will be very stiffly and linearly increased, and, however, if the element such as the center element of CANDU-6 fuel bundle has no neutron flux depression as well as has no variation of the coolant temperature and film heat transfer coefficient, there is no element bowing.

(8) With the increase of h_{fs} value only, the bowing of the asymmetric heat generating elements will be exponentially reduced, and, however, the bowing of the symmetric heat generating elements will be exponentially raised. The CANDU-6 asymmetric heat generated element bowing as an example is stiffly reduced in the range of $h_{fs} = 0.001$ to about 30kW/m²K, while the element bowing is slowly decreased in the range of hfs = about 30 to 90kW/m²K. The bowing of CANDU asymmetric or symmetric heat generating element will slowly and linearly reduced with the increase of α_s value only, and, however will be stiffly and linearly raised with the increase of a value only. With the increase of λ_s value only, the deflection of the asymmetric heat generating elements will be slowly and exponentially reduced, and, however, the deflection of the asymmetric and symmetric heat generating elements will be slowly and exponentially raised. The bowing of the asymmetric or symmetric heat generating elements will be slowly and linearly decreased with the increase of λ value only.

(9) Based on the above conclusions, it can be realized that the variations or changes of the element length, the sheath inner radius a, the average coolant temperature, the $\overline{T_c}$ oolant temperature variation factor β, the pellet/sheath mechanical interaction factor G, the neutron flux depression factor D, the element linear power q′, the pellet thermal expansion coefficient α, and the pellet/sheath heat transfer coefficient h_{fs} relatively effect in great on the element bowing than those of other parameters such as the sheath thickness t, the film heat transfer coefficient variation factor γ, the sheath thermal expansion coefficientα_s, the sheath and pellet thermal conductivities, λ_s and λ.

Nomenclatures

a and b	= inner and outer radii of sheath
D	= neutron flux gradient factor, defined in text
E and E_s	= Young's moduli of fuel and sheath
h_{fs}	= heat transfer coefficient between fuel and sheath
h_{sc} and $\overline{h_{sc}}$	= local and average film heat transfer coefficients between sheath and coolant
I_s	= moment of inertia for sheath
K_1 to K_4	= quantities defined in text.
l	= unrestrained length of fuel element
q′	= power per unit fuel length
r and θ	= cylindrical coordinates of point P with respect to axis of element (see Fig. 2)
R_i and R	= distances of element axis and point P from bundle axis (see Fig. 2)
t	= sheath thickness (= b − a)
$T(r, \theta)$	= temperature at point P
ΔT_s, ΔT_{sc}	= difference between maximum and minimum sheath surface temperatures in the individual and combined effects of non-mechanical and mechanical interactions between the pellet and the sheath
$\overline{T_c}$	= average coolant temperature
α and α_s	= thermal expansion coefficients of fuel and sheath
β, γ	= quantities defined in text relating to variation of coolant temperatures and film heat transfer coefficient

δ = magnitude of bow

κ = inverse diffusion length for thermal neutrons in homogenized bundle (fuel, sheath and coolant)

λ and λ_s = thermal conductivities of fuel and sheath

References

1. J. Veeder and M.H. Schankula, "Bowing of Pelletized Fuel Element-Theory and In-Reactor Experiments", Nuclear Engineering and Design 29 (1974)
2. M. Tayal, "Modelling the Bending/Bowing of Composite Beam such as Nuclear Fuel: The BOW Code", Nuclear Engineering and Design 116 (1989)
3. H.C. Suk, K-S. Sim, J.H. Park, G.S. Park, T.S. Byun, C.J. Jeong "Re-Derivation and Assessment of Thermally-Induced Fuel Element Bowing for BOW Code", KAERI Report, KAERI-TR-493/94, February (1995)
4. P.M. Morese and H. Feshaback, "Methods of Theoretical Physics", McGraw-Hill Book Company, Inc. New York (1953)
5. J.B. Marion, "Classical Electromagnetic Radiation", Academic Press, New York (1965)
6. B.A. Boley and J.H. Weiner, "Theory of Thermal Stress", John Wiley & Sons, Inc., New York (1960)
7. M. Gacesa, V.C. Orpan and I.E. Oladaker, "CANDU Fuel Design: Current Concept" Presented at IAEA/CENA International Semina on Heavy Water Fuel Technology, San Carlos de Bariloche, June 27-July 1 (1983)
8. D.S. Rowe, "COBRA IIIC, a Digital Computer Program for Steady-State and Transient Thermal-Hydraulic of a Rod Bundle Nuclear Fuel Elements", BNWL-1695, Battelle Richland, Washington, March (1973)
9. J.V. Donnelly, "WIMS-AECL, a User's Manual for the Chalk River Version of WIMS", AECL report, AECL-8955 (1986)
10. M. Tayal, "Modelling CANDU Fuel under Normal Operating Conditions; ELESTRES Code Description", AECL report, AECL-9331, February (1987)